On Interference Pikes in Poisson Networks

Mahin K. Atiq[1], Udo Schilcher[1,2], and Christian Bettstetter[1]
[1]Institute of Networked and Embedded Systems, University of Klagenfurt, Austria
[2]Lakeside Labs GmbH, Klagenfurt am Wörthersee, Austria

***Abstract*—The temporal dynamics of interference power is studied in Poisson networks with slotted random access and Rayleigh fading. Specifically, we analyze the occurrence of high interference events (*pikes*) and the time in between (*valleys*). Our main insight is that pikes arrive in bursts. This observation may help in the design of reliability techniques.**

***Index Terms*—Interference, fading, Poisson networks, wireless**

I. Introduction

The modeling and characterization of fading channels is a well-studied field in communications engineering. A channel's space-time dynamics can be described by various properties, such as coherence time, decorrelation distance, average fade duration (AFD), and level crossing rate (LCR). These characteristics are essential in the design of communication techniques: the decorrelation distance determines the antenna placement in multi-antenna systems, while the coherence time, AFD, and LCR are used to select interleaver depth, symbol duration, slot duration, and packet length [1]. Deep fading events hold particular interest, where the reception power falls below the receiver sensitivity or other relevant thresholds.

In an interference-limited scenario, the problem is reciprocal, whereby events of high interference rather than low-power periods are critical. Some expressions for the space-time dynamics of interference are available (e.g., interference correlation and interference coherence time [2–4]), but an analysis of high interference events along with the corresponding LCR and duration — i.e., how often the interference changes from low to high (and vice versa) and how long it remains high (or low) — has not been conducted thus far. In this paper, we contribute to this field by investigating the occurrence and duration of events of high interference (we call them *pikes*) and the time between these events (*valleys*). The categorization of interference into pikes and valleys is made using a *normalized threshold*, and the analysis is conducted for varying autocorrelation and mean power of interference. We focus on networks with Poisson distributed nodes that perform slotted message transmissions over a Rayleigh fading channel. The simulation results provide insights into the behavior of interference and may help to improve the design of reliability techniques, such as channel coding and interleaving. Our main insight is that pike events are not uniformly distributed over time but rather tend to occur in *bursts*. A potential generalization of this statement to other network models is subject to ongoing work.

The paper is organized as follows: Section II addresses related work. Section III presents the network model. Section IV analyzes interference pikes and valleys. Section V concludes.

II. Related Work

Work on the outage duration in communications over fading channels can be considered as related work. Expressions for LCR and AFD exist for selection combining and maximal ratio combining scheme over Rayleigh, Rice, and Nakagami fading channels [5; 6]. The LCR and AFD are also analyzed for a multi-hop relay network [7; 8]. However, co-channel interference is not considered in these results. Expressions for LCR and AFD in an amplify-and-forward relay network in the presence of co-channel interference with Rayleigh fading [9] and in interference-limited systems employing dual selection and equal gain combining [10; 11] are available. The AFD is analyzed for a general fading model, considering multi-hop communication systems [12]. For a Rayleigh fading channel, expressions for minimum outage duration are derived and analyzed [13]. In all of these results, only a few interferers are considered, and the correlation of interference is neglected.

III. Network Model

A static wireless network is given with nodes distributed by a Poisson point process (PPP) Φ with intensity λ. Time is divided into slots indexed by t. Each node $i \in \Phi$ starts the transmission of a message in a given slot independent of other nodes, with a probability p_i. A message is d_i slots long, and p_i is selected such that $p_i d_i \leq 1$. A Bernoulli random variable $\gamma_i(t)$ indicates whether node i is transmitting ($\gamma_i(t) = 1$) or not ($\gamma_i(t) = 0$) in slot t. The transmission power κ is the same for all nodes. The path loss from a node i at location x_i to a location x is $\ell_i = \min(1, \|x_i - x\|^{-\alpha})$, with a constant path loss exponent α. The multipath propagation effects are modeled by Rayleigh fading, represented by the i.i.d. exponen-

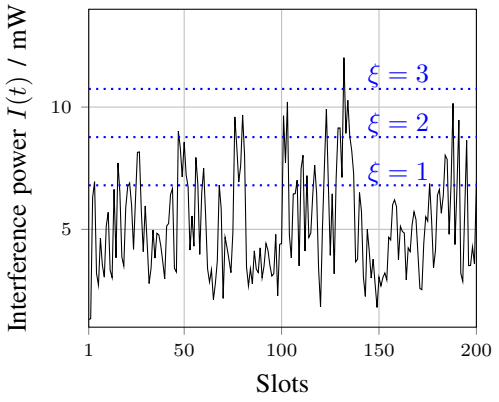

Fig. 1: Interference power at origin with different thresholds.

978-9-0827-9703-9/19/$31.00 ©2019 IEEE

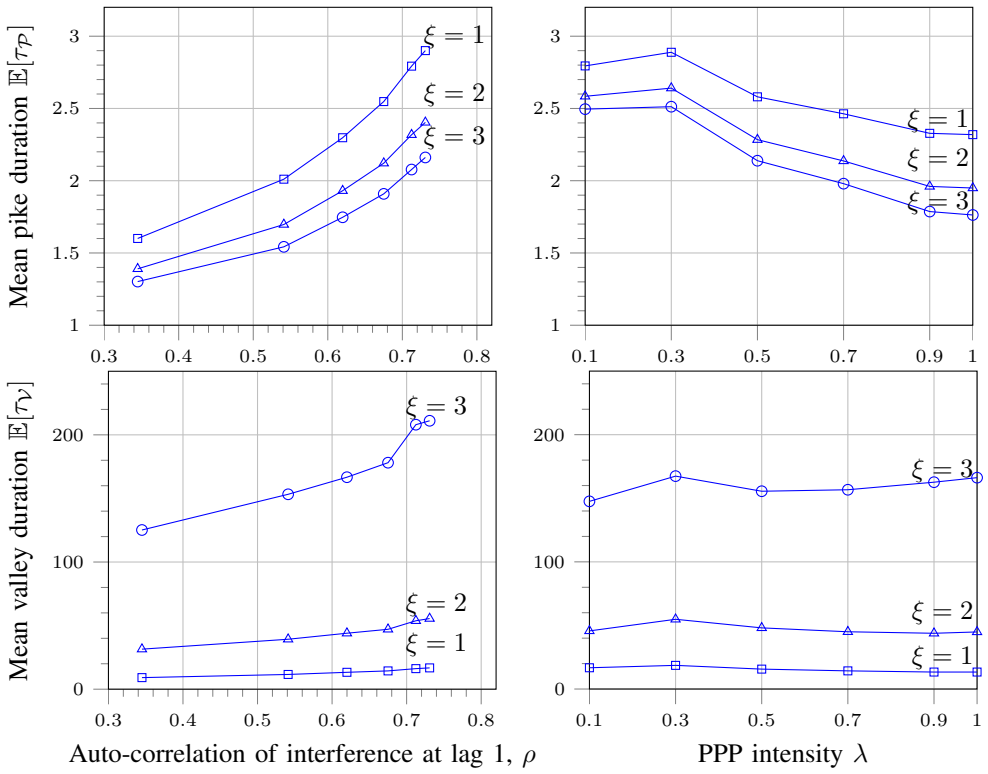

(a) Constant $\mathbb{E}[I(t)]$ with $\lambda = 1$

(b) Constant ρ with $\mathbb{E}[d_i] = 5$

Fig. 2: Mean duration of pikes and valleys. Parameters: $\mathbb{E}[p_i]\,\mathbb{E}[d_i] = 0.5$ and $c = 15$.

tially distributed variable $h_i^2(t)$. The channel remains constant for c slots and then changes to an independent value (block fading). This setup corresponds to case $(0, 2, 2)$ in [3]. We use $\lambda = 1$ m^{-2} and $\alpha = 3$.

IV. Interference Pikes and Valleys

The co-channel transmissions in slot t cause interference with power $I(t) = \sum_{i\in\Phi} \kappa\, \ell_i\, h_i^2(t)\, \gamma_i(t)$. This value is correlated over time as messages can exceed the slot length and the channel is correlated over multiple slots due to block fading. The interference power can be categorized as high or low based on a threshold θ between these two states. We employ a threshold that is normalized to the mean and standard deviation of $I(t)$. Specifically, we use $\theta = \mathbb{E}[I(t)] + \xi\, \sigma_{I(t)}$ [14], where $\sigma_{I(t)}$ is the standard deviation of $I(t)$ and $\xi \in \mathbb{N}$ is a scaling parameter, which determines the level of interference with which a receiver can cope. Fig. 1 shows a sample trace of $I(t)$ with three different thresholds.

The pike duration $\tau_\mathcal{P}$ is the number of consecutive slots with $I(t) > \theta$. Reciprocally, the valley duration $\tau_\mathcal{V}$ is the number of consecutive slots with $I(t) \leq \theta$. The interarrival time between pikes is given by a full pike-valley period $(\tau_\mathcal{P} + \tau_\mathcal{V})$. We study a typical node and all nodes in a network.

A. Analysis of a typical node of the network

Nodes are distributed on an area $A = 100$ m $\times$ 100 m. Due to the stationarity of the PPP, the interference experienced by a typical node of the network is the same as the one at the origin ($x = 0$). The message length d_i is chosen from an exponential distribution with parameter η, rounded up to the next integer and remaining constant for a given node, which yields a mean message length of $\mathbb{E}[d_i] = \frac{e^\eta}{e^\eta - 1}$. The results are averaged over 100 realizations of Φ and 100,000 slots.

Two setups are considered. First, we keep $\mathbb{E}[I(t)]$ constant and vary the autocorrelation ρ of interference, which is achieved by varying $\mathbb{E}[d_i]$ while adjusting $\mathbb{E}[p_i]$ correspondingly to keep the fraction of active nodes at $\mathbb{E}[p_i]\,\mathbb{E}[d_i] = 0.5$. Second, we keep ρ constant and vary $\mathbb{E}[I(t)]$, which is implemented by keeping $\mathbb{E}[d_i]$ and $\mathbb{E}[p_i]$ fixed but varying λ, which leads to a constant ρ because λ does not influence ρ [4].

Mean pike and valley durations: Fig. 2a shows the mean values of $\tau_\mathcal{P}$ and $\tau_\mathcal{V}$ for constant $\mathbb{E}[I(t)]$. With growing $\mathbb{E}[d_i]$, the fraction of nodes sending in consecutive slots increases while $\mathbb{E}[p_i]$ decreases. This results in longer pikes and valleys with increasing ρ. Fig. 2b shows the results for constant ρ. Increasing λ makes the pikes slightly shorter and keeps the valleys almost unchanged. This is because $\mathbb{E}[I(t)]$ and $\sigma_{I(t)}$ increase with λ, but the normalized threshold balances this effect across the plot. In both setups, the pikes become shorter and the valleys longer if we increase the threshold.

Distribution of pike and valley durations: After the mean values, we analyze the empirical probability mass functions (pmf) of $\tau_\mathcal{P}$ and $\tau_\mathcal{V}$. The scaling parameter is set to $\xi = 1$ in the following. Fig. 3a shows the pmfs for constant $\mathbb{E}[I(t)]$.

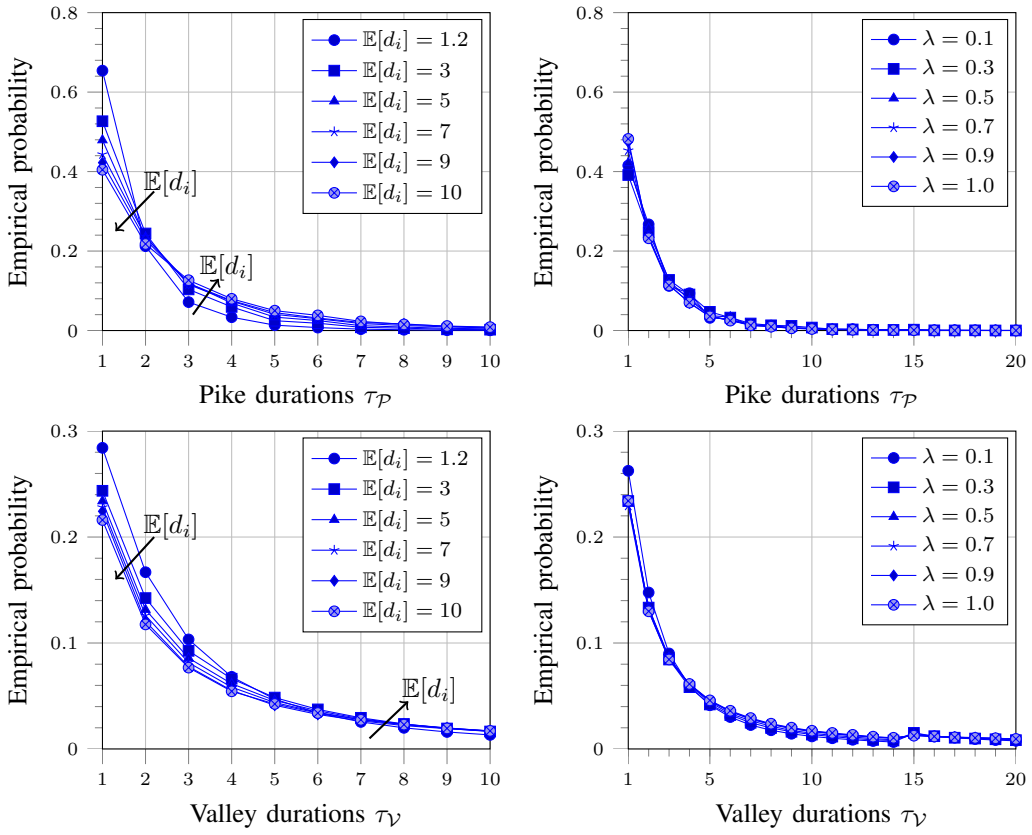

(a) Constant $\mathbb{E}[I(t)]$ with $\lambda = 1$

(b) Constant ρ with $\mathbb{E}[d_i] = 5$

Fig. 3: Empirical probability of pike and valley duration. Parameters: $\mathbb{E}[p_i]\,\mathbb{E}[d_i] = 0.5$, $c = 15$, and $\xi = 1$.

Short pikes and short valleys are more likely than long ones. The constant $\mathbb{E}[I(t)]$ leads to a constant fraction of time in which $I(t)$ exceeds θ. Thus, the very probable short valleys need to be compensated by improbable long valleys. The likelihood of short pikes and valleys increases with a decreasing message length $\mathbb{E}[d_i]$, i.e., with increasing $\mathbb{E}[p_i]$ and decreasing ρ. Fig. 3b shows the results for constant ρ. Again, short pikes and valleys occur with higher probability than long ones. The probabilities slightly increase at $\tau_{\mathcal{V}} = 15$ due to the channel block length being $c = 15$. The distributions are rather independent of λ due to the normalized θ.

Fig. 4 compares some of these pmfs with a geometric distribution with the same mean $\mathbb{E}[\tau_{\mathcal{P}}]$ and $\mathbb{E}[\tau_{\mathcal{V}}]$, respectively. In the considered range, the geometric distribution has a lower (higher) probability of short (long) durations. A comparison using constant ρ yields a similar behavior (plots not shown).

Distribution of pike interarrival time: Fig. 5 shows for a given node placement the events when $I(t)$ crosses θ, either upwards (from low to high interference) or downwards (vice versa). This example illustrates that the crossing moments are not uniformly distributed in time but rather arrive in bursts, i.e., sometimes there are several short pikes in a row followed by a long valley (and several short valleys followed by a long pike). The pmf of the interarrival time of pikes for constant $\mathbb{E}[I(t)]$ compared with a geometric distribution given in Fig. 6 confirms this non-Poisson arrival behavior. Short and very long interarrival times are more likely than in the geometric distribution and medium interarrival times are less likely.

B. Analysis of all nodes of a network

Let us finally adopt a network perspective. We employ a traffic model in which all nodes transmit for a fixed span of time (thus $d_i = d$ is constant for all nodes i) and each idle node starts a new message in a given slot with probability $p_i = p$, where $pd = 0.5$. This setting helps us to understand the spatial dependence of $\tau_{\mathcal{P}}$ and $\tau_{\mathcal{V}}$, since all nodes experience the same traffic volume. Fig. 7 shows the fraction of time with interference above θ, the mean pike durations, and the mean valley durations. Averaging is conducted over 100,000 slots. The color of a node indicates its neighbor count, i.e., the number of nodes in a unit circle around it.

The results are as follows: Both $\mathbb{E}[\tau_{\mathcal{P}}]$ and the fraction of time with interference above θ increase with the neighbor count (Fig. 7a and 7b). By contrast, $\mathbb{E}[\tau_{\mathcal{V}}]$ decreases with increasing neighbor count (Fig. 7c). Nodes with the same neighbor count (same color) have similar results and therefore accumulate in the plot.[1] For increasing d, the fraction of time

[1]We exclude nodes with single or few pikes during the simulation time, as their $\mathbb{E}[\tau_{\mathcal{V}}]$ is much higher and we want to focus on the overall behavior of the network. These outliers are also excluded from the overall mean.

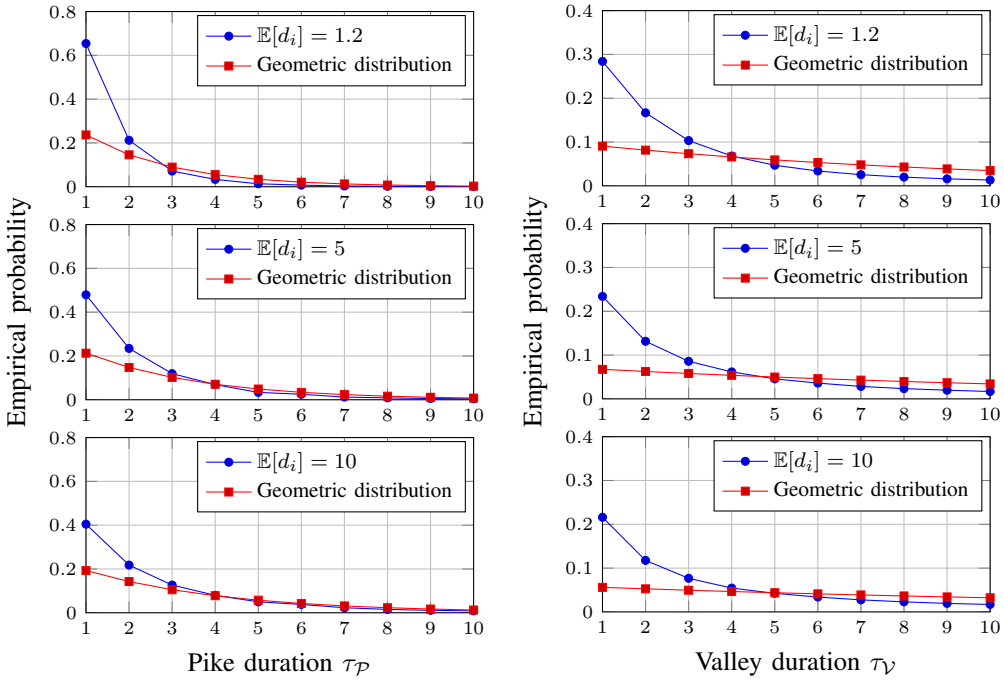

Fig. 4: Comparison of distribution of pike and valley durations with the geometric distribution for constant $\mathbb{E}[I(t)]$. Parameters: $\mathbb{E}[p_i]\,\mathbb{E}[d_i] = 0.5$, $c = 15$, $\lambda = 1$ and $\xi = 1$.

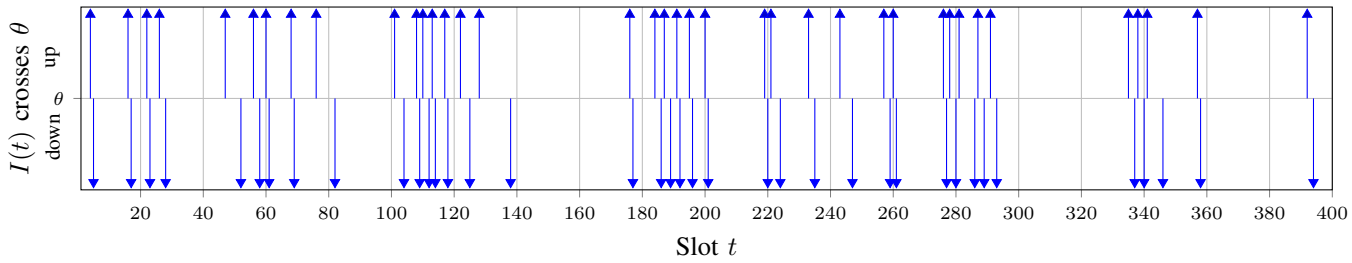

Fig. 5: Events when the interference power crosses the threshold θ (upwards and downwards). Parameters: $\mathbb{E}[p_i] = 0.1$, $\mathbb{E}[d_i] = 5$, $c = 15$, $\lambda = 1$ and $\xi = 1$.

above θ remains constant, whereas $\mathbb{E}[\tau_{\mathcal{P}}]$ increases. This can be explained by the constant pd and the intuition that for longer messages a closeby interferer will keep interference above θ for a longer time. By contrast, $\mathbb{E}[\tau_{\mathcal{V}}]$ does not show this effect, since the idle periods of the interferers are not quantized by d.

V. Conclusions and Outlook

In Poisson networks with Rayleigh block fading and the given traffic model, the level crossings between low and high interference occur in bursts. This insight may support the design of reliability techniques, in a similar way as we exploit the coherence time of the channel to mitigate burst errors in the design of interleavers. Further work is necessary to assess other types of node distribution, channel, and traffic models and derive analytical expressions.

Acknowledgments

This work has been supported by the Austrian Science Fund (FWF) under grant P24480-N15 (Dynamics of Interference in Wireless Networks) and by the K-project DeSSnet. The K-project DeSSnet is funded within the context of COMET—Competence Centers for Excellent Technologies—by the Austrian Ministry for Transport, Innovation and Technology (BMVIT), the Federal Ministry for Digital and Economic Affairs (BMDW), and the federal states of Styria and Carinthia. The program is conducted by the Austrian Research Promotion Agency (FFG).

References

[1] M. K. Simon and M.-S. Alouini, *Digital communication over fading channels*. Wiley-IEEE press, Dec. 2005.

[2] R. K. Ganti and M. Haenggi, "Spatial and temporal correlation of the interference in ALOHA ad hoc networks," *IEEE Commun. Lett.*, vol. 13, no. 9, pp. 631–633, 2009.

[3] U. Schilcher, C. Bettstetter, and G. Brandner, "Temporal correlation of interference in wireless networks with Rayleigh block fading," *IEEE Trans. Mobile Comput.*, vol. 11, no. 12, pp. 2109–2120, 2012.

[4] U. Schilcher, J. F. Schmidt, M. K. Atiq, and C. Bettstetter, "Auto-correlation and coherence time of interference in Poisson networks," *IEEE Trans. on Mobile Comput.*, 2019.

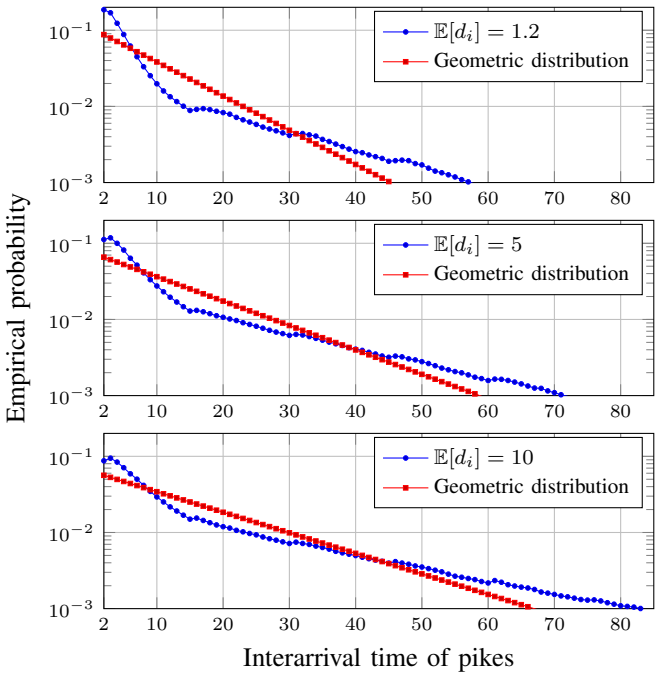

Fig. 6: Comparison of distribution of interarrival time of pikes with the geometric distribution for constant $\mathbb{E}[I(t)]$. Parameters: $\mathbb{E}[p_i]\,\mathbb{E}[d_i] = 0.5$, $c = 15$, $\lambda = 1$ and $\xi = 1$.

[5] X. Dong and N. C. Beaulieu, "Average level crossing rate and average fade duration of selection diversity," *IEEE Commun. Lett.*, vol. 5, no. 10, pp. 396–398, 2001.

[6] A. Olutayo, H. Ma, J. Cheng, and J. F. Holzman, "Level crossing rate and average fade duration for the Beaulieu-Xie fading model," *IEEE Commun. Lett.*, vol. 6, pp. 326–329, 2017.

[7] F. J. Lopez-Martinez, E. Kurniawan, R. Islam, and A. Goldsmith, "Average fade duration for amplify-and-forward relay networks in fading channels," *IEEE Trans. Wireless Commun.*, vol. 14, no. 10, pp. 5454–5467, 2015.

[8] A. A. Gebremichail and C. Beard, "Multi-hop relay selection based on fade durations," in *Proc. Wirel. Telecom. Symp.*, 2015.

[9] M. S. Gilan, M. Y. Manesh, and A. Mohammadi, "Level crossing rate and average fade duration of amplify and forward relay channels with cochannel interference," in *Proc. European Wireless*, 2016.

[10] Z. Hadzi-Velkov, "Level crossing rate and average fade duration of dual selection combining with cochannel interference and Nakagami fading," *IEEE Trans. Wireless Commun.*, vol. 6, no. 11, pp. 3870–3876, 2007.

[11] Z. Hadzi-Velkov, "Level crossing rate and average fade duration of EGC systems with cochannel interference in Rayleigh fading," *IEEE Trans. Commun.*, vol. 55, no. 11, pp. 2104–2113, 2007.

[12] L. Yang, M. O. Hasna, and M.-S. Alouini, "Average outage duration of multihop communication systems with regenerative relays," *IEEE Trans. Wireless Commun.*, vol. 4, no. 4, pp. 1366–1371, 2005.

[13] J. Lai and N. B. Mandayam, "Minimum duration outages in Rayleigh fading channels," *IEEE Trans. Commun.*, vol. 49, no. 10, pp. 1755–1761, 2001.

[14] F. Pukelsheim, "The three sigma rule," *The American Statistician*, vol. 48, no. 2, pp. 88–91, 1994.

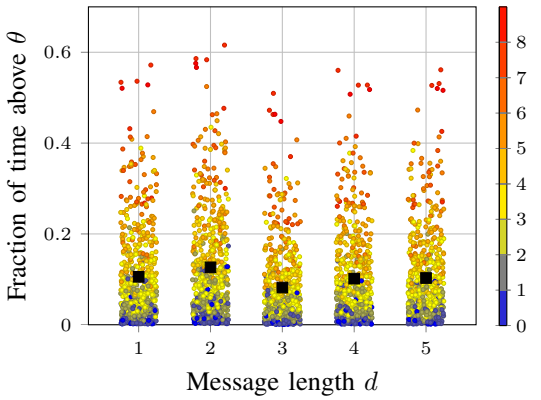

(a) Fraction of time above θ.

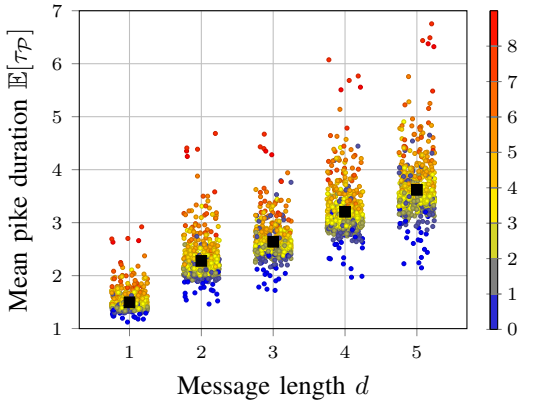

(b) Mean pike duration $\mathbb{E}[\tau_{\mathcal{P}}]$.

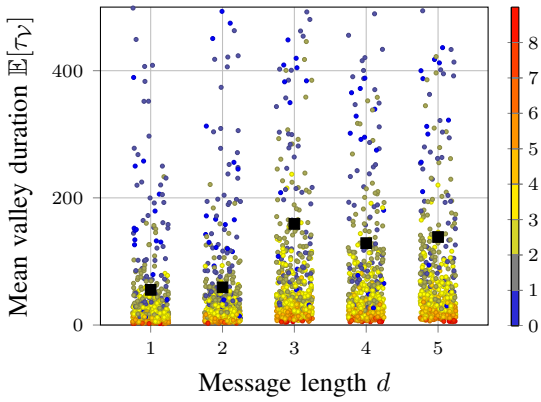

(c) Mean valley duration $\mathbb{E}[\tau_{\mathcal{V}}]$.

Fig. 7: Analysis for all nodes of a network. The color of each node represents its neighbor count. A jitter is added across the x-axis to visually separate the colored points. Mean values are shown as solid black square markers. Parameters: $pd = 0.5$, $c = 15$, $\lambda = 1$, $\xi = 1$, and $A = 625$ m^2.